Journal of Controlled Release xxx (2014) xxx–xxx

Contents lists available at ScienceDirect

Journal of Controlled Release

journal homepage: www.elsevier.com/locate/jconrel

Theranostic nanoparticles for future personalized medicine

Q1 Ju Hee Ryu [a], Sangmin Lee [a], Sohee Son [a], Sun Hwa Kim [a], James F. Leary [b], Kuiwon Choi [a], Ick Chan Kwon [a,c,*]

[a] Center for Theragnosis, Biomedical Research Institute, Korea Institute of Science and Technology (KIST), Hwarangno 14-gil 6, Seongbuk-gu, Seoul 136-791, Republic of Korea
[b] Basic Medical Sciences and Biomedical Engineering, Bindley Bioscience Center and Brick Nanotechnology Center, Purdue University, West Lafayette 47907, USA
[c] KU-KIST School, Korea University, 1 Anam-dong, Seongbuk-gu, Seoul 136-701, Republic of Korea

ARTICLE INFO

Article history:
Received 11 February 2014
Accepted 12 April 2014
Available online xxxx

Keywords:
Theranostics
Personalized medicine
Molecular imaging
Monitoring response

ABSTRACT

The concept of personalized medicine has recently emerged as a promising way to address unmet medical needs. Due to the limitations of standard diagnostic and therapeutic strategies, the disease treatment is moving towards tailored treatment for individual patients, considering the inter-individual variability in therapeutic response. Theranostics, which involves the combination of therapy and diagnostic imaging into a single system, may fulfill the promise of personalized medicine. By integrating molecular imaging functionalities into therapy, theranostic approach could be advantageous in therapy selection, treatment planning, objective response monitoring and follow-up therapy planning based on the specific molecular characteristics of a disease. Although the field of therapy and imaging of its response have been independently developed thus far, developing imaging strategies can be fully exploited to revolutionize the theranostic systems in combination with the therapy modality. In this review, we describe the recent advances in molecular imaging technologies that have been specifically developed to evaluate the therapeutic efficacy for theranostic purposes.

© 2014 Published by Elsevier B.V.

1. Introduction

The paradigm for the disease treatment is changing; clinicians are gradually going beyond the traditional "one-size-fits-all" approach of medicine toward a new era of personalized treatment strategies [1,2]. In such approaches, medical treatments are tailored to the specific characteristics of individual patients [3]. No single therapeutic agent is recognized to produce the same effect in different patients with a single type of disease. Considering the inter-individual variability in therapeutic response, a patient-specific treatment may produce better therapeutic outcomes, while reducing patient discomfort and undesirable side-effects [4].

Theranostics, the integration of therapeutic and diagnostic capability in a single system, may contribute significantly to the ever-growing field of personalized medicine [5]. By combining molecular imaging functionalities with therapy, a theranostic approach could be advantageous in identifying and selecting a particular subgroup of patients with a specific molecular phenotype. A particular molecular phenotype can be an indication of positive response to a certain treatment. This is especially significant because treatment using monoclonal antibodies, such as cetuximab and trastuzumab is increasing. In addition, this approach can serve as a valuable tool in the selection of a safe and efficacious dose, recognition of adverse effects at the early stages of therapy, and real-time objective monitoring of the therapeutic response [6]. For example, clinicians can switch to other therapeutic options, or they can adjust the therapeutic dose for non-responders to the current therapeutic regimen, while continuing the therapy for good responders.

In particular, nanotechnology could be applied advantageously to theranostics [7]. The most commonly used nano-sized materials for theranostic purposes are polymeric nanoparticle, lipid-based nanoparticle, dendrimer, cage protein and inorganic nanoparticle [8–10]. These nano-sized particles (NPs) provide numerous advantages for the theranostic applications. One of the greatest advantageous characteristics of NPs is their potential to localize in pathological lesions more than normal lesions *in vivo*, particularly in the case of cancer [11,12]. NPs can easily extravasate from blood vessels into tumor tissues because of leaky and irregularly dilated blood vessels at the tumor site, and they can be retained at tumor sites owing to poor lymphatic drainage. This phenomenon of selective accumulation of NPs near tumor tissues is termed the enhanced permeability and retention (EPR) effect [13,14], allowing their targeted imaging and therapy. In addition to cancer, EPR-like effect is known to be observed in the inflammation region because various immunocytes release vasodilators and chemotactic factors in the inflammation region [15–17]. Another promising characteristic of NPs is their large surface-area-to-volume ratio; this allows for a high loading capacity of imaging probes, therapeutic drugs, or targeting moieties [18,19]. NPs with multiple functions can remarkably benefit monitoring treatment progress and evaluating outcomes, because they can be used to diagnose and track certain

* Corresponding author at: Center for Theragnosis, Biomedical Research Institute, Korea Institute of Science and Technology (KIST), Hwarangno 14-gil 6, Seongbuk-gu, Seoul 136-791, Republic of Korea. Tel.: +82 2 958 5912; fax: +82 2 958 5909.
E-mail address: ikwon@kist.re.kr (I.C. Kwon).

http://dx.doi.org/10.1016/j.jconrel.2014.04.027
0168-3659/© 2014 Published by Elsevier B.V.

Please cite this article as: J.H. Ryu, et al., Theranostic nanoparticles for future personalized medicine, J. Control. Release (2014), http://dx.doi.org/10.1016/j.jconrel.2014.04.027

molecular targets of highly heterogeneous diseases such as cancer with multiple-targeting possibilities and sensitive imaging capabilities [20, 21].

For theranostic purposes, a variety of nanomaterials such as polymers and silica have been extensively investigated. These nanomaterials have been utilized for loading both imaging agents and drugs. Polymer-based NPs are the most widely investigated theranostic nanoplatform. Polymer-based NPs, usually fabricated by the self-assembly of amphiphilic polymers, can load hydrophobic drugs or imaging agents in the inner cores or functionalize their surface with imaging agents or targeting moieties. These encapsulating and surface-modifying properties of polymer-based NPs mean that they can potentially serve as prospective theranostic agents [22]. Furthermore, silica-based NPs are advantageous in terms of their well-established siloxane chemistry and well-defined tunable nanostructures. These properties allow for the effective fabrication of a desired surface in the silica-based NPs for therapeutic and diagnostic applications [11]. Besides classical drug delivery systems such as polymer-based NPs and silica-based NPs, many nanomaterials including iron oxide or gold-based NPs have intrinsic imaging abilities, which can further be loaded with drugs for theranostics. Iron oxide-based NPs can be noninvasively imaged by magnetic resonance (MR) imaging and utilized for drug delivery, which makes them a potential theranostic nanoplatform. To prevent the aggregation of iron oxide-based NPs in biological media, the modification of their surface with hydrophilic polymers such as dextran is preferred. Gold-based NPs have been widely researched as multifunctional agents for theranostic purposes because they have distinctive optical characteristics and unique photothermal properties along with low toxicity and well-established gold chemistry.

Theranostic NPs simultaneously carrying both imaging probes and therapeutic agents were primarily utilized to investigate drug delivery process and drug release pattern [23]. Theranostic approaches to drug response monitoring remain in their developmental stages up to date, and the integration of therapy and the imaging of its response into one theranostic system has not yet been studied in detail. In this review, we describe recent imaging strategies that have been specifically developed for the evaluation of the therapeutic efficacy for theranostic purposes.

2. Treatment with theranostic NPs

Theranostic NPs can be applied for cancer therapy including chemotherapy, siRNA therapy, and photodynamic therapy. Some small-molecule drugs have disadvantages including toxic side effects in normal tissues, insufficient specificity to tumor tissues, limited delivery to tumor cells owing to their hydrophobicity, and drug-resistance [7]. Theranostic NPs have the potential to solve these problems in traditional chemotherapy [24,25]. Furthermore, a theranostic NP delivery system can be beneficial for siRNA therapy. Theranostic NPs can be effective at enhancing the stability of siRNA in the blood stream after intravenous injection, minimizing degradation by many enzymes. Considering that naked siRNA can be eliminated from the blood within 5 min after intravenous injection, prolonged circulation time of siRNA in NPs can contribute to effective therapy. In addition, negatively charged siRNA cannot easily enter the cytosol of target cells, which can be overcome by theranostic NPs for siRNA therapy [26–28]. In the case of photodynamic therapy, theranostic NP-based photodynamic therapy affords advantages including reduced systemic toxicity and improved solubility in water compared to classical photodynamic therapy. The selective accumulation of photosensitizers contained in NPs inside the target can significantly lower the systemic toxicity related to classical photodynamic therapy. In addition, most photosensitizers used in photodynamic therapy can aggregate in biological media, leading to a change in their optical properties [29].

3. Imaging modalities for theranostics

In theranostic approaches, diagnostic imaging is essential for determining the presence and degree of molecular targets for a certain disease [30,31]. Presently, various noninvasive imaging modalities can be applied to visualize molecular targets *in vivo*: optical imaging, ultrasound (US) imaging, MR imaging, computed tomography (CT) and nuclear imaging (single photon emission computed tomography (SPECT) and positron emission tomography (PET)). These modalities can be broadly separated into primarily molecular imaging modalities and primarily morphological/anatomical imaging modalities [32]. The former, which are characterized by high sensitivity, include optical imaging and PET/SPECT; on the other hand, the latter, which are featured by high spatial resolution, include CT, US and MR [32,33]. The detailed advantages and disadvantages of individual imaging modalities would be left out because they have been previously discussed in many literatures [4,34]. In particular, optical imaging and PET/SPECT have great potential to detect molecular targets that are important in a disease process; thus, they are more favorable for theranostic approaches. In more recent, integrated molecular/anatomical systems (e.g., SPECT/CT) have been developed to combine the strengths of individual imaging modalities [35,36].

4. Monitoring certain molecular targets involved in disease progression

Targeted molecular imaging, an essential component of a theranostic system, can be used to image and track molecular targets involved in disease progression. Noninvasive molecular imaging can be used to identify the presence and degree of molecular targets through a whole-body scan in real time, which is valuable in disease staging and therapy planning such as drug dosage and timing. For example, most chemotherapeutic agents, such as doxorubicin (DOX), exert their effects by inducing apoptosis, which is the process of programmed cell death. Therefore, detecting and quantifying apoptosis would be useful for monitoring the chemotherapeutic efficacy. A useful approach for assessing apoptosis is to monitor the specific molecules involved in apoptosis signaling. Caspases are a group of cysteine proteases that play key roles in apoptosis [37]. They convey the signal in apoptotic caspase cascades by cleaving and amplifying multiple caspases through various pathways, which ultimately contributes to cell death [38]. Among various caspases, caspase-3 is widely recognized as an important and direct mediator of apoptosis [39]. Our group developed nanoprobes for detecting caspase-3 activity [40]. This nanoprobe consists of hyaluronic acid-based polymeric nanoparticles (HA-NPs) and a caspase-3 substrate peptide-based probe (Fig. 1). The peptide-based probe comprises Cy5.5, a near infrared (NIR) dye, and black hole quencher-3 (BHQ-3), a dark quencher, covalently linked to both end parts of a short peptide (Gly-Asp-Glu-Val-Asp-Ala-Pro-Lys-Gly-Cys) that can serve as a hydrolyzable substrate for caspase-3 (Fig. 1A). The synthesized peptide-based probe is conjugated onto the surface of HA-NPs to afford Cas3-HA-NP (Fig. 1A, B). The NIR dye is strongly dual-quenched because of the dye–dye quenching and dye–quencher interaction mechanisms, contributing to reduced background signals. In the presence of caspase-3, Cas3-HA-NP showed the linear proportional recovery of NIR fluorescence signals depending on the caspase-3 concentration *in vitro* (Fig. 1C). Cas3-HA-NP was activated to produce a strong high-resolution fluorescence signal in real time in apoptotic cells induced by the tumor necrosis factor-related apoptosis-inducing ligand (TRAIL). NIR fluorescence signals produced by Cas3-HA-NP were detected as early as 15 min post-treatment of TRAIL; in contrast, annexin V staining, the current gold standard target for evaluating apoptosis, yielded apoptosis signals 1 h post-treatment (Fig. 1D). In addition, Cas3-HA-NP enabled clear *in vivo* visualization of apoptosis induced by DOX in tumor-bearing mice (Fig. 1E–G). NIR fluorescence signals produced by Cas3-HA-NP were well-matched with apoptosis signals analyzed by the

UNCORRECTED PROOF

Please cite this article as: J.H. Ryu, et al., Theranostic nanoparticles for future personalized medicine, J. Control. Release (2014), http://dx.doi.org/10.1016/j.jconrel.2014.04.027

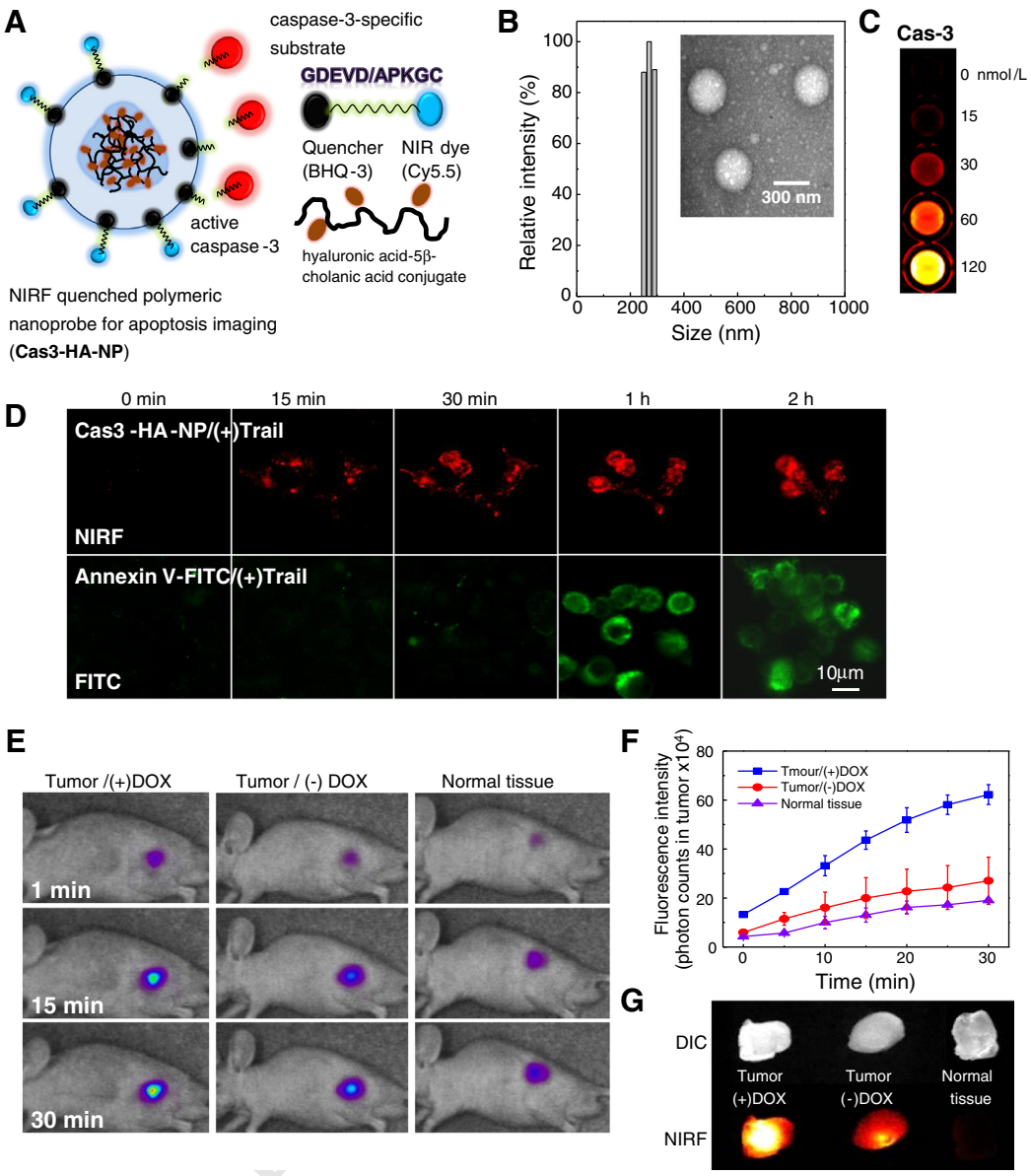

Q9 **Fig. 1.** Fluorescence-activatable nanoprobe, and cellular and *in vivo* caspase-3 imaging. (A) Schematic diagram of caspase-3-sensitive nanoprobe (Cas3-HA-NP). (B) Size distribution and morphological shape (TEM image) of the Cas3-HA-NPs. (C) Fluorescence image of a 96-well microplate containing the Cas3-HA-NPs in the presence of various concentrations of caspase-3. (D) Real time video imaging of caspase-3 activity in HCT116 cells using the Cas3-HA-NPs. Cells were incubated with the Cas3-HA-NPs (20 μg/mL) for 30 min, and then treated with tumor necrosis factor-related apoptosis inducing ligand (TRAIL, 100 ng/mL). Apoptosis of cells treated with TRAIL was also evaluated by the annexin V-FITC staining. (E) *In vivo* near-infrared fluorescence imaging of subcutaneous SCC7 tumor-bearing mice after intratumoral injection of the Cas3-HA-NPs with or without pretreatment of doxorubicin (DOX). (F) Quantitative analysis by counting total photons in the Cas3-HA-NP-treated tumor tissues as a function of time ($n = 5$). (G) *Ex vivo* tumor tissue images from (E).

terminal deoxynucleotidyl transferase dUTP nick end labeling (TUNEL) assay, which is used to detect apoptosis in dissected tumor tissues. Therefore, this imaging probe (Cas3-HA-NP) can be applied to monitor the therapeutic response and efficacy of apoptosis-related drugs in cancer therapy. Importantly, this imaging probe platform for detecting proteases is so flexible that it can be applied to different proteases by simply changing the cleavable substrate peptide [41–44].

Recently, a more multiplexed system (MultiCas-NP) has been devised to target three types of caspases (caspase-3, -8 and -9) involved in apoptotic signaling cascades (Fig. 2) [45]. This nanoprobe is based on a nanoquencher system comprising mesoporous silica NPs incorporated into a series of dark quenchers to quench a variety of dyes (Fig. 2A). Different caspase-specific substrate peptides linked with various dyes were conjugated onto the surface of the nanoquencher system for the simultaneous detection of caspase-3, -8 and -9. As expected, various caspases activated specific substrate peptides linked with the dye, producing the particular signals of the corresponding dye (Fig. 2B, C). MultiCas-NP boosted multiplexed fluorescence intensities in the presence of multiple caspases in a single apoptotic cell induced by TRAIL (Fig. 2D). More importantly, MultiCas-NP has great potential for *in vivo* use to monitor the efficacy of apoptosis-related treatment in individual patients in real time. These imaging probes for monitoring particular molecular targets involved in disease progression can be used to revolutionize theranostic systems in combination with the therapy modality.

5. Monitoring downstream molecular targets affected by treatment

The efficacy of a treatment can be evaluated by monitoring certain molecules in a downstream process affected by the treatment as well as the targeted molecules of the treatment. In addition to chemotherapeutic drugs, small interference RNA (siRNA) has attracted considerable attention as a potential therapy for the treatment of various diseases,

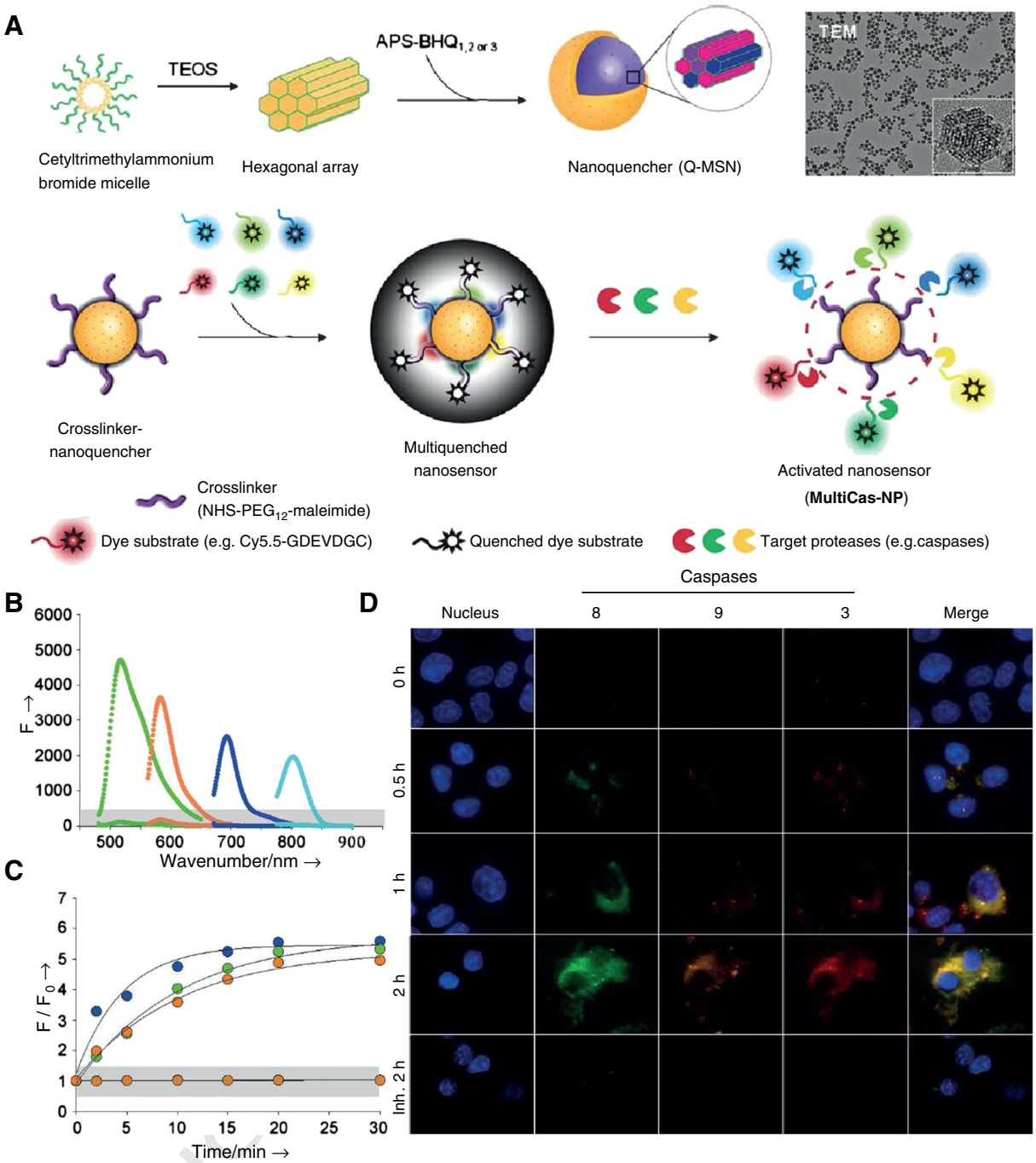

Fig. 2. Multiplex fluorescence-activatable nanoprobe for caspase cascade imaging. (A) Schematic diagram of various caspases (caspase-3, -8, and -9)-sensitive multiplex nanoprobe (MultiCas-NP). Image: TEM image of the nanoquenchers (Q-MSNs). (B) Fluorescence-quenching properties of Q-MSNs concurrently labeled with FPG-456 (green), FPR-560 (orange), Cy5.5 (dark blue), and FPI-774 (light blue). Upper lines = fluorescence emission spectra of free fluorescence dyes; lower lines in gray zone = emission spectra of fluorescence dyes after quenching by Q-MSNs. (C) The relative increase in fluorescence (F/F_0) of MultiCas-NPs in the presence (upper lines) or absence (lower lines, gray zone) of caspase-3 (blue), caspase-8 (green), or caspase-9 (orange). (D) Multiplex imaging of the caspase cascade in HCT116 cells. Blue (DAPI) = nucleus; green (FPG456) = caspase-8; purple (FPG560) = caspase-9; red (Cy5.5) = caspase-3; inh. = with inhibitor. (For interpretation of the references to color in this figure legend, the reader is referred to the web version of this article.)

especially owing to its specific therapeutic effects [46,47]. The action mechanism of siRNA is post-transcriptional gene silencing by cleavaging the target mRNA that shares a homologous sequence with the treated siRNA [48,49]. This sequence specific suppression of targeted gene can be utilized for efficient therapy through the decrease of targeted molecules related with the disease [50].

Our group reported thiolated glycol chitosan (tGC) nanoparticles encapsulating tumor necrosis factor (TNF)-α targeted polymerized siRNA (poly-siRNA) for the treatment of rheumatoid arthritis (RA) (Fig. 3) [17]. Among a variety of proinflammatory cytokines associated in the pathogenesis of RA, TNF-α plays a major role to induce chronic inflammation via stimulating the release of multiple cytokines and other inflammatory mediators (Fig. 3A) [51,52]. Therefore, TNF-α inhibition has been an important target for RA treatment [53,54]. Poly-siRNA, prepared through the self-polymerization of thiol groups at the 5′ end of their sense and antisense strands, can be easily encapsulated into tGC polymers through charge–charge interaction and chemical cross-linking to produce psi-tGC-NPs (Fig. 3B–D) [55–57]. The TNF-α-targeted siRNA loaded psi-tGC-NPs exhibited excellent *in vitro* gene silencing for TNF-α and significant *in vivo* inhibition of inflammation and bone erosion in

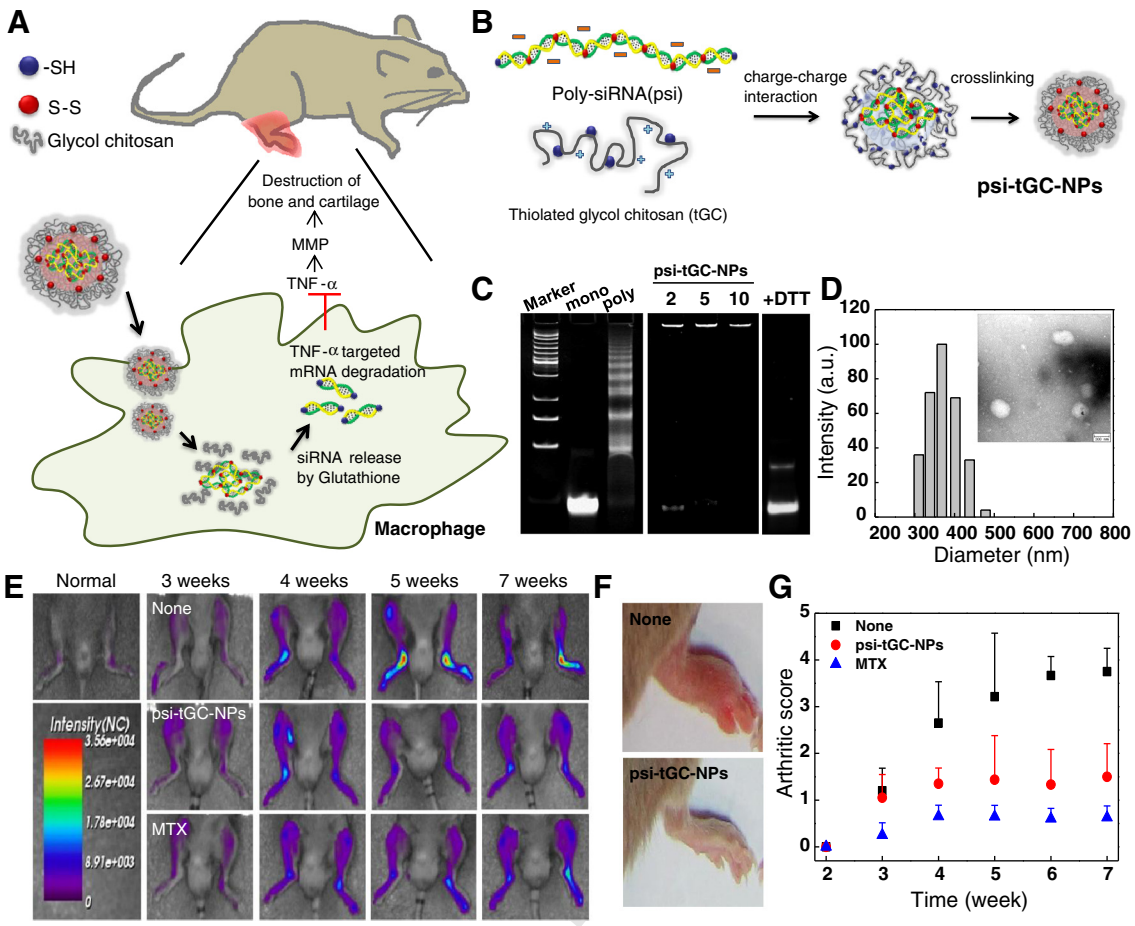

Fig. 3. Polymerized siRNA/thiolated glycol chitosan nanoparticles (psi-tGC-NPs) for rheumatoid arthritis (RA) therapy. (A) Schematic diagram of psi-tGC-NPs for tumor necrosis factor (TNF)-α targeted siRNA delivery in RA therapy. (B) Complexation of poly-siRNA with tGC polymers. (C) Confirmation of poly-siRNA formation by gel electrophoresis of mono- or poly-siRNA and gel retardation of complexes of thiolated GC with poly-siRNA (psi-tGC-NPs) at different weight ratios (1:2, 1:5, and 1:10 tGC/siRNA). +DTT: Reduction of poly-siRNA by adding 1,4-dithiothreitol (DTT). (D) Size distribution and morphological shape (TEM image) of the psi-tGC-NPs. (E) *In vivo* near-infrared fluorescence imaging of normal mice and arthritis mice in each group (untreated (none), psi-tGC-NP-treated, and methotrexate (MTX)-treated) after intravenous injection of MMP-3 nanoprobe (MMP-3-NP) at different stages of disease (at 3, 4, 5, and 7 weeks after the primary immunization) for monitoring of the disease progression in arthritis mice. (F) The paw swelling in each group of (E). (G) Arthritic score in each group of (E).

collagen-induced arthritis mouse models, as evaluated by microCT or immunoblot analysis (Fig. 3E–G). Importantly, disease progression following psi-tGC-NP therapy was evaluated by monitoring of matrix metalloproteinase-3 (MMP-3) in a downstream process affected by the therapy using *in vivo* NIR fluorescence imaging (Fig. 3E). MMPs have been known to play a pivotal role in persistent synovial inflammation and articular cartilage degradation, both of which are early symptoms of RA [58]. Among several MMPs related in these processes, MMP-3 is recognized to be particularly significant in the pathogenesis of RA [59]. MMP-3 is known to degrade many proteins of matrices, including collagens, proteoglycans, gelatins, laminin and fibronectin [59]. More interestingly, MMP is known to be downregulated by inhibiting TNF-α in arthritic progression [60,61]. This probe for detecting MMP-3 consists of the same platform as Cas3-HA-NP, which is described above. The MMP-3 substrate peptide-based probe comprises cleavable substrate peptide (Gly-Val-Pro-Leu-Ser-Leu-Thr-Met-Gly-Lys-Gly-Gly), Cy5.5, and BHQ-3. These peptide-based probes are then conjugated onto the surface of glycol chitosan NPs, to afford MMP-3-NP. In our previous study, the NIR fluorescence signal from MMP-3-NP was apparently able to indicate the presence and severity of arthritic disease [16]. Significantly reduced NIR fluorescence signals from MMP-3-NP were observed in the psi-tGC-NPs-treated group compared with the untreated control group in collagen-induced arthritic mice. Therefore, monitoring a molecular target in a downstream process affected by the treatment can be a potential approach for assessing the clinical effectiveness of the treatment.

6. Using a nanostructure similar to therapeutic vehicles

A nanostructure identical to that used for drug treatment can be loaded with an imaging agent for the real-time visualization of drug efficacy. Following the treatment using a nanostructure loaded with a therapeutic agent, a structurally identical nanostructure labeled with an imaging agent can be applied to monitor the therapeutic response. At first, this theranostic approach has been applied to receptor-targeting radiolabeled peptides and not nanostructures. For instance, somatostatin receptors that are over-expressed in many neuroendocrine tumors can bind to a specific peptide sequence with high binding affinity [62]. Thus, somatostatin receptor-binding peptides labeled with a therapeutic (β-emitting) radionuclide (^{177}Lu) could eradicate somatostatin-receptor-positive endocrine tumors. In particular, somatostatin receptor-binding peptides labeled with a diagnostic (γ-emitting) radionuclide (^{111}In) for SPECT could visualize binding sites in receptor-expressing neuroendocrine tumors in a non-invasive manner, allowing the monitoring of the progress and outcome after surgery, radiotherapy, or chemotherapy. In addition, patients with a neuroendocrine pancreatic tumor were diagnosed using ^{111}In-octreotide, a radiolabeled somatostatic analogue, after three radionuclide therapy cycles using ^{177}Lu-octreotate [63]. They used octreotide and octreotate as target peptides with high affinity particularly for somatostatic receptor type 2. In SPECT imaging, no discernible uptake was observed in the tumor sites after three radionuclide

therapy cycles, revealing the good therapeutic efficacy of radionuclide therapy.

Recently, our group reported that a nanostructure similar to a therapeutic one can be useful for the real-time visualization of treatment efficacy (Fig. 4). A PEGylated hyaluronic acid nanoparticle (P-HA-NP) was utilized for the early diagnosis, targeted therapy and chemotherapeutic monitoring of colon cancer in tumor model [64]. P-HA-NPs encapsulating irinotecan (IRT), an anticancer drug, selectively targeted tumors through the EPR effect of NPs and strong receptor-binding to CD44, overexpressing receptors in various tumors (Fig. 4A). As a result, the P-HA-NP encapsulating IRT (P-HA-NP–IRT)-treated group exhibited significant inhibition of tumor growth compared to the free IRT or saline-treated groups, as confirmed through measurements of the tumor size (Fig. 4B). To monitor the therapeutic response, Cy5.5 was conjugated onto the surface of P-HA-NPs (Cy5.5–P-HA-NPs). Indeed, the fluorescence intensity of Cy5.5–P-HA-NPs in the P-HA-NP–IRT-treated group was notably lower than that in the free IRT or saline-treated groups, which is attributed to the decreased accumulation of Cy5.5–P-HA-NPs at tumor sites by a combination of passive targeting (EPR effect) and active targeting (CD44 binding) in the case of suppressed tumor growth (Fig. 4C) [65, 66]. Using a nanostructure identical to that used for treatment for diagnostic purposes can be useful not only for monitoring the therapeutic response but also for selecting patients who will benefit from an identical nanostructure loaded with a therapeutic agent. If the presence of imaging agents (Cy5.5 attachment onto the NP surface) and therapeutic agents (IRT loading into NP) does not affect the shape, size and surface features of the nanostructure, specific pharmacokinetics and biodistribution of diagnostic nanostructures in individual patients can be identical to those of therapeutic nanostructures [67]. Therefore, patient-specific treatment seems possible by varying the biodistribution and pharmacokinetics of the therapeutic nanostructure.

The integration of therapy and imaging of its response into one theranostic system was described in chitosan-based NPs (CNPs) (Fig. 5) [68]. Different formulations of PTX–CNPs were prepared by loading with different amounts of PTX (5, 10, or 20 mg PTX/kg) and by labeling with Cy5.5 (Cy5.5–CNP–PTX) (Fig. 5A, B). In these formulations, loaded PTX amounts were adjusted to be correlated with the NIR fluorescence intensity of each NP. Therefore, how much PTX can be delivered to the tumor sites in SCC7 tumor-bearing mouse models can be visualized by NIR fluorescence signals. Strong NIR fluorescence signals in the tumors were displayed with the frequency of injections at three-day intervals; thus determining optimal protocol is administration of Cy5.5–CNP–PTX at three-day intervals (Fig. 5C). PTX–CNPs treated with this optimal administration protocol resulted in the improved reduction in tumor volume compared to treatment of free PTX (Fig. 5D, E). A standard for determining optimal protocol in this study was the drug concentration in the tumor sites. If therapy was integrated with the imaging functionalities to evaluate drug efficacy into one theranostic system, drug efficacy can be a standard for deciding the optimal drug dosage in question, enhancing both safety and effectiveness of the drug.

7. Conclusions

This review describes recent imaging strategies that have been specifically developed for evaluating the therapeutic efficacy for theranostic purposes. Diagnostic imaging utilizing certain molecular targets involved in disease progression, downstream molecular targets affected by treatment, and a nanostructure similar to a therapeutic one could potentially be used to evaluate the therapeutic response and efficacy during or after treatment. Unfortunately, the current status of theranostic technology for drug response monitoring has remained in the developmental stage; thus far, few studies have focused on the integration of therapy and its response imaging into one theranostic system. However, the call for a more personalized approach to medical treatment and extensive ongoing developments in nanotechnology together with diagnostic imaging strategies discussed in this review

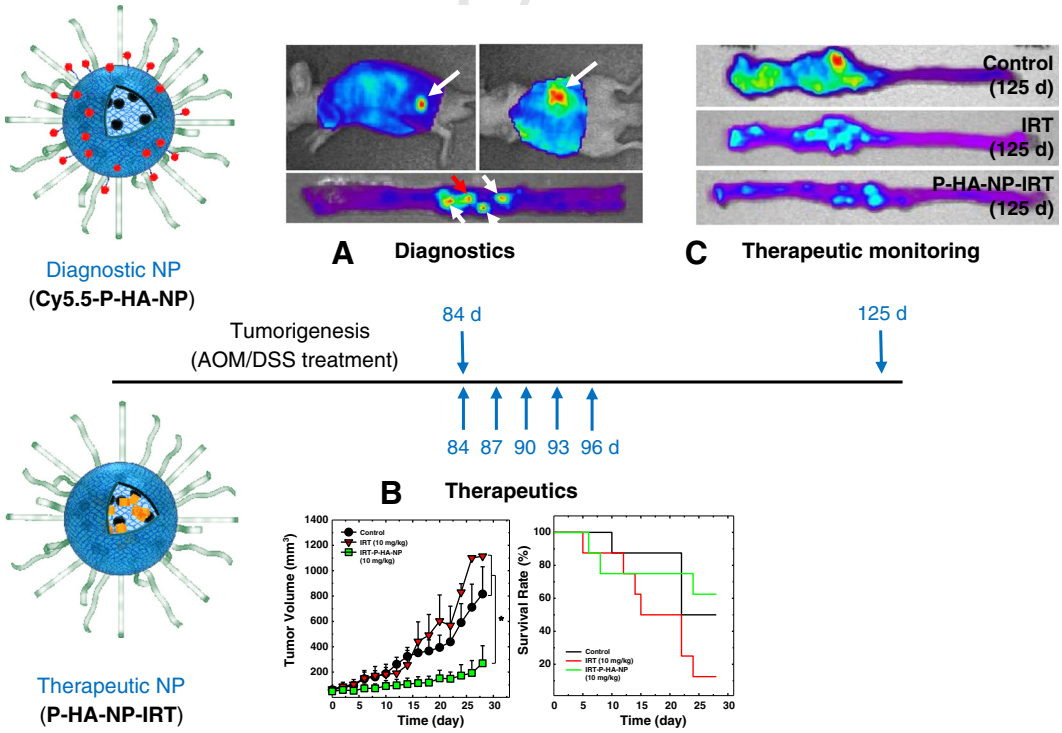

Fig. 4. PEGylated hyaluronic acid nanoparticles (P-HA-NPs) for the diagnosis, therapy, and chemotherapeutic monitoring of colon cancer. (A) Diagnostics: *In vivo* near-infrared (NIR) fluorescence imaging of small-sized HT29 flank tumors (top-left), liver-implanted CT26 colon tumors (top-right), and early stage orthotopic colon tumors (bottom) after intravenous injection of Cy5.5 conjugated to P-HA-NPs (Cy5.5–P-HA-NPs). Arrows indicate the sites of tumors. (B) Therapeutics: Tumor growth and survival rate of human colon cancer (HT29) xenografts treated with saline, free irinotecan (IRT), and IRT-encapsulated P-HA-NPs (P-HA-NPs–IRT) at a dose of 10 mg IRT/kg. (C) Therapeutic monitoring: Representative colon images of orthotopic colon cancer models after treatment of saline, IRT, or P-HA-NPs–IRT. NIR fluorescence images were acquired at 6 h after intravenous injection of Cy5.5–P-HA-NPs.

Please cite this article as: J.H. Ryu, et al., Theranostic nanoparticles for future personalized medicine, J. Control. Release (2014), http://dx.doi.org/10.1016/j.jconrel.2014.04.027

ARTICLE IN PRESS

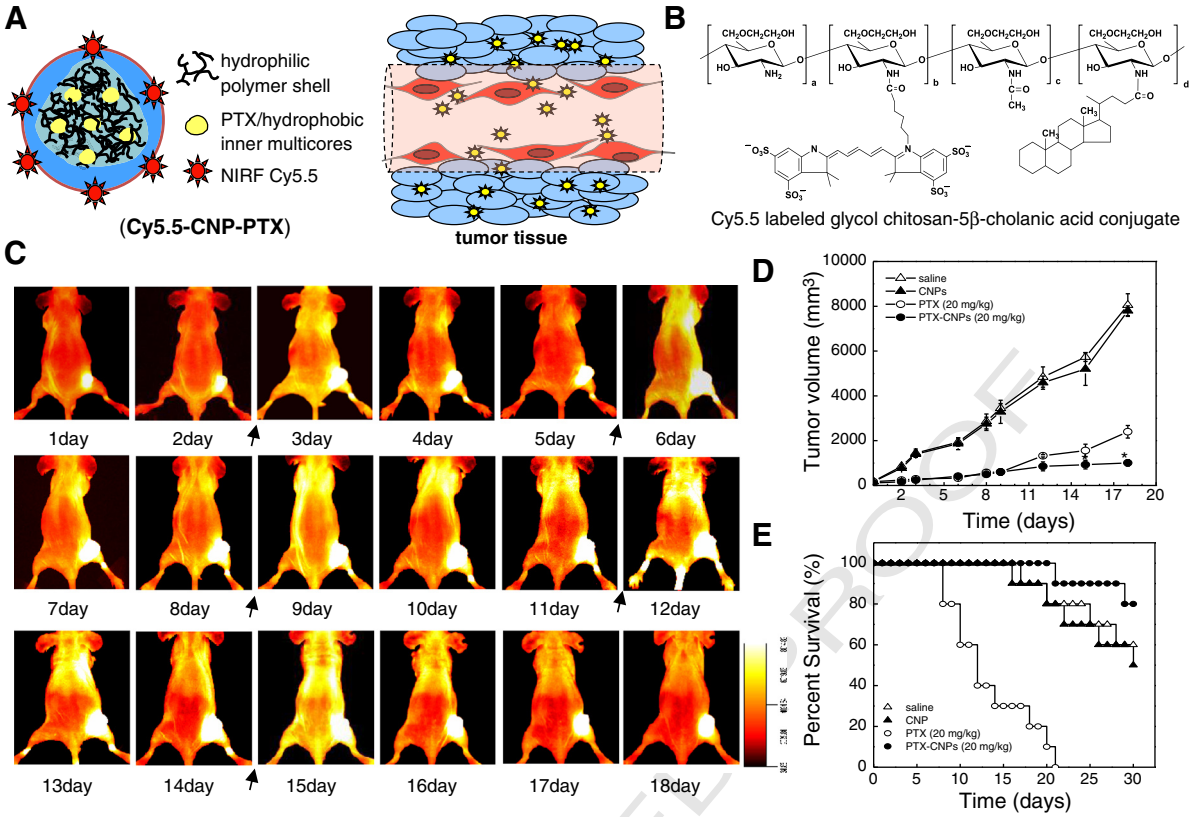

Fig. 5. Theranostic chitosan-based nanoparticles (CNPs) for simultaneous diagnosis, chemotherapy, and therapeutic monitoring of cancer. (A) Schematic diagram of self-assembled CNPs labeled with Cy5.5 for imaging and therapeutic monitoring, and encapsulated with paclitaxel (PTX) for chemotherapy (Cy5.5–CNPs–PTX). (B) Chemical structure of glycol chitosan–cholanic acid conjugates labeled with Cy5.5. (C) *In vivo* near-infrared fluorescence imaging of tumor specificity and tumor growth rate in Cy5.5–CNPs–PTX (20 mg PTX/kg)-injected SCC7 tumor bearing mice. The black arrows indicate intravenous injection of Cy5.5–CNPs–PTX. (D) Therapeutic efficacy of PTX–CNPs in SCC7 tumor-bearing mice. (E) Survival curves.

might revolutionize to theranostic systems in the near future. Some important issues, however, must be preferentially resolved to achieve successful integration into theranostic systems. In particular, theranostic systems need to improve the apparent mismatch between the optimal concentrations of imaging agents and therapeutic agents for potential clinical use, since the optimal concentration for a desired therapy is generally much higher than that required for imaging. Furthermore, a theranostic system can contain multiple functions within an individual system, and this may increase the complexity of the system. Thus, the development of reproducible and simple methods for designing theranostic systems can help in achieving the successful integration of imaging and therapy. In addition, to accelerate the clinical translation of theranostic NP, utilizing clinically validated nanomaterials could lower the risk of translation [69]. Diagnostic imaging for monitoring therapeutic efficacy has been shown to play an important role in many ways of personalized medicine. The development of diagnostic imaging following treatment, desirably in a single system, could enable therapy selection, treatment planning, objective response monitoring and follow-up therapy planning based on the specific molecular characteristics of a disease, thus paving the way for personalized medicine.

Acknowledgments

This study was funded by the National Research Foundation of Korea (NRF-2013K1A1A2032346 and 2012K1A1A2A01056095) and the Intramural Research Program (Theragnosis) of KIST.

References

[1] N.B. La Thangue, D.J. Kerr, Predictive biomarkers: a paradigm shift towards personalized cancer medicine, Nat. Rev. Clin. Oncol. 8 (2011) 587–596.
[2] M. Diamandis, N.M.A. White, G.M. Yousef, Personalized medicine: marking a new epoch in cancer patient management, Mol. Cancer Res. 8 (2010) 1175–1187.
[3] M. Kalia, Personalized oncology: recent advances and future challenges, Metabolism 62 (Supplement 1) (2013) S11–S14.
[4] J.V. Jokerst, S.S. Gambhir, Molecular imaging with theranostic nanoparticles, Acc. Chem. Res. 44 (2011) 1050–1060.
[5] T.H. Kim, S. Lee, X. Chen, Nanotheranostics for personalized medicine, Expert. Rev. Mol. Diagn. 13 (2013) 257–269.
[6] G. Bartlett, J. Antoun, N.K. Zgheib, Theranostics in primary care: pharmacogenomics tests and beyond, Expert. Rev. Mol. Diagn. 12 (2012) 841–855.
[7] J.H. Ryu, H. Koo, I.-C. Sun, S.H. Yuk, K. Choi, K. Kim, I.C. Kwon, Tumor-targeting multifunctional nanoparticles for theragnosis: new paradigm for cancer therapy, Adv. Drug Deliv. Rev. 64 (2012) 1447–1458.
[8] A. Puri, R. Blumenthal, Polymeric lipid assemblies as novel theranostic tools, Acc. Chem. Res. 44 (2011) 1071–1079.
[9] B. Sumer, J. Gao, Theranostic nanomedicine for cancer, Nanomedicine 3 (2008) 137–140.
[10] H. Koo, M.S. Huh, I.-C. Sun, S.H. Yuk, K. Choi, K. Kim, I.C. Kwon, *In vivo* targeted delivery of nanoparticles for theranosis, Acc. Chem. Res. 44 (2011) 1018–1028.
[11] C.M. Wang LS, J.A. Ho, Nanotheranostics—a review of recent publications, Int. J. Nanomedicine 7 (2012) 4679–4695.
[12] I. Brigger, C. Dubernet, P. Couvreur, Nanoparticles in cancer therapy and diagnosis, Adv. Drug Deliv. Rev. 54 (2002) 631–651.
[13] H. Maeda, Macromolecular therapeutics in cancer treatment: the EPR effect and beyond, J. Control. Release 164 (2012) 138–144.
[14] H. Maeda, H. Nakamura, J. Fang, The EPR effect for macromolecular drug delivery to solid tumors: improvement of tumor uptake, lowering of systemic toxicity, and distinct tumor imaging *in vivo*, Adv. Drug Deliv. Rev. 65 (2013) 71–79.
[15] Y.-N. Chang, H. Guo, J. Li, Y. Song, M. Zhang, J. Jin, G. Xing, Y. Zhao, Adjusting the balance between effective loading and vector migration of macrophage vehicles to deliver nanoparticles, PLoS ONE 8 (2013) e76024.
[16] J.H. Ryu, A. Lee, J.-U. Chu, H. Koo, C.-Y. Ko, H.S. Kim, S.-Y. Yoon, B.-S. Kim, K. Choi, I.C. Kwon, K. Kim, I. Youn, Early diagnosis of arthritis in mice with collagen-induced arthritis, using a fluorogenic matrix metalloproteinase 3-specific polymeric probe, Arthritis Rheum. 63 (2011) 3824–3832.
[17] S.J. Lee, A. Lee, S.R. Hwang, J.-S. Park, J. Jang, M.S. Huh, D.-G. Jo, S.-Y. Yoon, Y. Byun, S.H. Kim, I.C. Kwon, I. Youn, K. Kim, TNF-[alpha] gene silencing using polymerized siRNA/thiolated glycol chitosan nanoparticles for rheumatoid arthritis, Mol. Ther. (2013).
[18] M.P. Melancon, R.J. Stafford, C. Li, Challenges to effective cancer nanotheranostics, J. Control. Release 164 (2012) 177–182.

Please cite this article as: J.H. Ryu, et al., Theranostic nanoparticles for future personalized medicine, J. Control. Release (2014), http://dx.doi.org/10.1016/j.jconrel.2014.04.027

ARTICLE IN PRESS

[19] J.D. Byrne, T. Betancourt, L. Brannon-Peppas, Active targeting schemes for nanoparticle systems in cancer therapeutics, Adv. Drug Deliv. Rev. 60 (2008) 1615–1626.
[20] S. Basu, Personalized versus evidence-based medicine with PET-based imaging, Nat. Rev. Clin. Oncol. 7 (2010) 665–668.
[21] V. Sanna, M. Sechi, Nanoparticle therapeutics for prostate cancer treatment, Nanomedicine: Nanotechnology, Biology and Medicine 8 (Supplement 1) (2012) S31–S36.
[22] S. Mura, P. Couvreur, Nanotheranostics for personalized medicine, Adv. Drug Deliv. Rev. 64 (2012) 1394–1416.
[23] T. Lammers, S. Aime, W.E. Hennink, G. Storm, F. Kiessling, Theranostic nanomedicine, Acc. Chem. Res. 44 (2011) 1029–1038.
[24] A. Khdair, C. Di, Y. Patil, L. Ma, Q.P. Dou, M.P.V. Shekhar, J. Panyam, Nanoparticle-mediated combination chemotherapy and photodynamic therapy overcomes tumor drug resistance, J. Control. Release 141 (2010) 137–144.
[25] T. Yoshitomi, Y. Ozaki, S. Thangavel, Y. Nagasaki, Redox nanoparticle therapeutics to cancer—increase in therapeutic effect of doxorubicin, suppressing its adverse effect, J. Control. Release 172 (2013) 137–143.
[26] R. Shrestha, M. Elsabahy, H. Luehmann, S. Samarajeewa, S. Florez-Malaver, N.S. Lee, M.J. Welch, Y. Liu, K.L. Wooley, Hierarchically assembled theranostic nanostructures for siRNA delivery and imaging applications, J. Am. Chem. Soc. 134 (2012) 17362–17365.
[27] K.A. Whitehead, R. Langer, D.G. Anderson, Knocking down barriers: advances in siRNA delivery, Nat. Rev. Drug Discov. 8 (2009) 129–138.
[28] F. Alexis, E. Pridgen, L.K. Molnar, O.C. Farokhzad, Factors affecting the clearance and biodistribution of polymeric nanoparticles, Mol. Pharm. 5 (2008) 505–515.
[29] P. Rai, S. Mallidi, X. Zheng, R. Rahmanzadeh, Y. Mir, S. Elrington, A. Khurshid, T. Hasan, Development and applications of photo-triggered theranostic agents, Adv. Drug Deliv. Rev. 62 (2010) 1094–1124.
[30] S.M. Janib, A.S. Moses, J.A. MacKay, Imaging and drug delivery using theranostic nanoparticles, Adv. Drug Deliv. Rev. 62 (2010) 1052–1063.
[31] M.F. Kircher, H. Hricak, S.M. Larson, Molecular imaging for personalized cancer care, Mol. Oncol. 6 (2012) 182–195.
[32] J.K. Willmann, N. van Bruggen, L.M. Dinkelborg, S.S. Gambhir, Molecular imaging in drug development, Nat. Rev. Drug Discov. 7 (2008) 591–607.
[33] Y. Huang, S. He, W. Cao, K. Cai, X.-J. Liang, Biomedical nanomaterials for imaging-guided cancer therapy, Nanoscale 4 (2012) 6135–6149.
[34] G. Kramer-Marek, J. Gore, M. Korc, Molecular imaging in pancreatic cancer—a roadmap for therapeutic decisions, Cancer Lett. 341 (2013) 132–138.
Q5 [35] M. de Smet, S. Langereis, S. van den Bosch, K. Bitter, N.M. Hijnen, E. Heijman, H. Grüll, SPECT/CT imaging of temperature-sensitive liposomes for MR-image guided drug delivery with high intensity focused ultrasound, J. Control. Release, 169 82–90
[36] A.E. John, J.C. Luckett, A.L. Tatler, R.O. Awais, A. Desai, A. Habgood, S. Ludbrook, A.D. Blanchard, A.C. Perkins, R.G. Jenkins, J.F. Marshall, Preclinical SPECT/CT imaging of αvβ6 integrins for molecular stratification of idiopathic pulmonary fibrosis, J. Nucl. Med. 54 (2013) 2146–2152.
[37] D.L. Vaux, S.J. Korsmeyer, Cell death in development, Cell 96 (1999) 245–254.
[38] M. Brentnall, L. Rodriguez-Menocal, R. De Guevara, E. Cepero, L. Boise, Caspase-9, caspase-3 and caspase-7 have distinct roles during intrinsic apoptosis, BMC Cell Biol. 14 (2013) 32.
[39] S.J. Riedl, Y. Shi, Molecular mechanisms of caspase regulation during apoptosis, Nat. Rev. Mol. Cell Biol. 5 (2004) 897–907.
[40] S. Lee, K.Y. Choi, H. Chung, J.H. Ryu, A. Lee, H. Koo, I.-C. Youn, J.H. Park, I.-S. Kim, S.Y. Kim, X. Chen, S.Y. Jeong, I.C. Kwon, K. Kim, K. Choi, Real time, high resolution video imaging of apoptosis in single cells with a polymeric nanoprobe, Bioconjug. Chem. 22 (2011) 125–131.
[41] S. Lee, J.H. Ryu, K. Park, A. Lee, S.-Y. Lee, I.-C. Youn, C.-H. Ahn, S.M. Yoon, S.-J. Myung, D.H. Moon, X. Chen, K. Choi, I.C. Kwon, K. Kim, Polymeric nanoparticle-based activatable near-infrared nanosensor for protease determination *in vivo*, Nano Lett. 9 (2009) 4412–4416.
[42] J.H. Ryu, J.H. Na, H.K. Ko, D.G. You, S. Park, E. Jun, H.J. Yeom, D.H. Seo, J.H. Park, S.Y. Jeong, I.-S. Kim, B.-S. Kim, I.C. Kwon, K. Choi, K. Kim, Non-invasive optical imaging of cathepsin B with activatable fluorogenic nanoprobes in various metastatic models, Biomaterials 35 (2014) 2302–2311.
[43] J.H. Ryu, S.A. Kim, H. Koo, J.Y. Yhee, A. Lee, J.H. Na, I. Youn, K. Choi, I.C. Kwon, B.-S. Kim, K. Kim, Cathepsin B-sensitive nanoprobe for *in vivo* tumor diagnosis, J. Mater. Chem. 21 (2011).
[44] J. Ryu, A. Lee, J. Na, S. Lee, H. Ahn, J. Park, C.-H. Ahn, B.-S. Kim, I. Kwon, K. Choi, I. Youn, K. Kim, Optimization of matrix metalloproteinase fluorogenic probes for osteoarthritis imaging, Amino Acids 41 (2011) 1113–1122.
[45] X. Huang, M. Swierczewska, K.Y. Choi, L. Zhu, A. Bhirde, J. Park, K. Kim, J. Xie, G. Niu, K.C. Lee, S. Lee, X. Chen, Multiplex imaging of an intracellular proteolytic cascade by using a broad-spectrum nanoquencher, Angew. Chem. Int. Ed. 51 (2012) 1625–1630.
[46] S. Yang, Y. Chen, R. Ahmadie, E.A. Ho, Advancements in the field of intravaginal siRNA delivery, J. Control. Release 167 (2013) 29–39.
[47] S. Zhang, B. Zhao, H. Jiang, B. Wang, B. Ma, Cationic lipids and polymers mediated vectors for delivery of siRNA, J. Control. Release 123 (2007) 1–10.
[48] H.Y. Yoon, H.R. Kim, G. Saravanakumar, R. Heo, S.Y. Chae, W. Um, K. Kim, I.C. Kwon, J. Y. Lee, D.S. Lee, J.C. Park, J.H. Park, Bioreducible hyaluronic acid conjugates as siRNA carrier for tumor targeting, J. Control. Release 172 (2013) 653–661.
[49] R. Kanasty, J.R. Dorkin, A. Vegas, D. Anderson, Delivery materials for siRNA therapeutics, Nat. Mater. 12 (2013) 967–977.
[50] M.E. Davis, J.E. Zuckerman, C.H.J. Choi, D. Seligson, A. Tolcher, C.A. Alabi, Y. Yen, J.D. Heidel, A. Ribas, Evidence of RNAi in humans from systemically administered siRNA via targeted nanoparticles, Nature 464 (2010) 1067–1070.
[51] M. Feldmann, R.N. Maini, TNF defined as a therapeutic target for rheumatoid arthritis and other autoimmune diseases, Nat. Med. 9 (2003) 1245–1250.
[52] Y. Komano, N. Yagi, I. Onoue, K. Kaneko, N. Miyasaka, T. Nanki, Arthritic joint-targeting small interfering RNA-encapsulated liposome: implication for treatment strategy for rheumatoid arthritis, J. Pharmacol. Exp. Ther. 340 (2012) 109–113.
[53] J.-L. Davignon, M. Hayder, M. Baron, J.-F. Boyer, A. Constantin, F. Apparailly, R. Poupot, A. Cantagrel, Targeting monocytes/macrophages in the treatment of rheumatoid arthritis, Rheumatology 52 (2013) 590–598.
[54] A. Alghasham, Z. Rasheed, Therapeutic targets for rheumatoid arthritis: Progress and promises, Autoimmunity, 0 1–18. Q6
[55] S.J. Lee, M.S. Huh, S.Y. Lee, S. Min, S. Lee, H. Koo, J.-U. Chu, K.E. Lee, H. Jeon, Y. Choi, K. Choi, Y. Byun, S.Y. Jeong, K. Park, K. Kim, I.C. Kwon, Tumor-homing poly-siRNA/glycol chitosan self-cross-linked nanoparticles for systemic siRNA delivery in cancer treatment, Angew. Chem. Int. Ed. 51 (2012) 7203–7207.
[56] S.J. Lee, J.Y. Yhee, S.H. Kim, I.C. Kwon, K. Kim, Biocompatible gelatin nanoparticles for tumor-targeted delivery of polymerized siRNA in tumor-bearing mice, J. Control. Release 172 (2013) 358–366.
[57] S. Son, S. Song, S.J. Lee, S. Min, S.A. Kim, J.Y. Yhee, M.S. Huh, I. Chan Kwon, S.Y. Jeong, Y. Byun, S.H. Kim, K. Kim, Self-crosslinked human serum albumin nanocarriers for systemic delivery of polymerized siRNA to tumors, Biomaterials 34 (2013) 9475–9485.
[58] I. Tchetverikov, L.R. Lard, J. DeGroot, N. Verzijl, J.M. TeKoppele, F.C. Breedveld, T.W.J. Huizinga, R. Hanemaaijer, Matrix metalloproteinases-3, -8, -9 as markers of disease activity and joint damage progression in early rheumatoid arthritis, Ann. Rheum. Dis. 62 (2003) 1094–1099.
[59] M.D. Posthumus, P.C. Limburg, J. Westra, H.A. Cats, R.E. Stewart, M.A. van Leeuwen, M.H. van Rijswijk, Serum levels of matrix metalloproteinase-3 in relation to the development of radiological damage in patients with early rheumatoid arthritis, Rheumatology 38 (1999) 1081–1087.
[60] A.I. Catrina, J. Lampa, S. Ernestam, E. Af Klint, J. Bratt, L. Klareskog, A.K. Ulfgren, Anti-tumour necrosis factor (TNF)-α therapy (etanercept) down-regulates serum matrix metalloproteinase (MMP)-3 and MMP-1 in rheumatoid arthritis, Rheumatology 41 (2002) 484–489. Q7
[61] A. Lee, Y. Qiao, G. Grigoriev, J. Chen, K.-H. Park-Min, S.H. Park, L.B. Ivashkiv, G.D. Kalliolias, Tumor necrosis factor α induces sustained signaling and a prolonged and unremitting inflammatory response in rheumatoid arthritis synovial fibroblasts, Arthritis Rheum. 65 (2013) 928–938.
[62] M. van Essen, A. Sundin, E.P. Krenning, D.J. Kwekkeboom, Neuroendocrine tumours: the role of imaging for diagnosis and therapy, Nat. Rev. Endocrinol. (2013) (advance online publication). Q8
[63] M. de Jong, W.A.P. Breeman, D.J. Kwekkeboom, R. Valkema, E.P. Krenning, Tumor imaging and therapy using radiolabeled somatostatin analogues, Acc. Chem. Res. 42 (2009) 873–880.
[64] K.Y. Choi, E.J. Jeon, H.Y. Yoon, B.S. Lee, J.H. Na, K.H. Min, S.Y. Kim, S.-J. Myung, S. Lee, X. Chen, I.C. Kwon, K. Choi, S.Y. Jeong, K. Kim, J.H. Park, Theranostic nanoparticles based on PEGylated hyaluronic acid for the diagnosis, therapy and monitoring of colon cancer, Biomaterials 33 (2012) 6186–6193.
[65] K.Y. Choi, H.Y. Yoon, J.-H. Kim, S.M. Bae, R.-W. Park, Y.M. Kang, I.-S. Kim, I.C. Kwon, K. Choi, S.Y. Jeong, K. Kim, J.H. Park, Smart nanocarrier based on PEGylated hyaluronic acid for cancer therapy, ACS Nano 5 (2011) 8591–8599.
[66] J.-H. Park, H.-J. Cho, H.Y. Yoon, I.-S. Yoon, S.-H. Ko, J.-S. Shim, J.-H. Cho, J.H. Park, K. Kim, I.C. Kwon, D.-D. Kim, Hyaluronic acid derivative-coated nanohybrid liposomes for cancer imaging and drug delivery, J. Control. Release 174 (2014) 98–108.
[67] S. Svenson, Theranostics: are we there yet? Mol. Pharm. 10 (2013) 848–856.
[68] K. Kim, J.H. Kim, H. Park, Y.-S. Kim, K. Park, H. Nam, S. Lee, J.H. Park, R.-W. Park, I.-S. Kim, K. Choi, S.Y. Kim, K. Park, I.C. Kwon, Tumor-homing multifunctional nanoparticles for cancer theragnosis: simultaneous diagnosis, drug delivery, and therapeutic monitoring, J. Control. Release 146 (2010) 219–227.
[69] J. Shi, Z. Xiao, N. Kamaly, O.C. Farokhzad, Self-assembled targeted nanoparticles: evolution of technologies and bench to bedside translation, Acc. Chem. Res. 44 (2011) 1123–1134.

UNCORRECTED PROOF

Please cite this article as: J.H. Ryu, et al., Theranostic nanoparticles for future personalized medicine, J. Control. Release (2014), http://dx.doi.org/10.1016/j.jconrel.2014.04.027